Int. J. Ion Mobil. Spec. (2010) 13:109–119
DOI 10.1007/s12127-010-0048-3

ORIGINAL RESEARCH

Performance of stacked, flow-through micropreconcentrators for portable trace detection

Michael D. Martin · Thomas J. Roussel · Scott Cambron · Julia Aebersold · Douglas Jackson · Kevin Walsh · Ji-Tzuoh Lin · Martin G. O'Toole · Robert Keynton

Received: 25 August 2010 / Revised: 27 September 2010 / Accepted: 28 September 2010 / Published online: 13 October 2010

Abstract Improving techniques for portable trace analyte collection and pretreatment is of critical concern for security, medical, food and environmental applications. The trend has been to employ MEMS technologies to meet this need as these microfabricated devices offer advantages such as small dead volumes, low power consumption, capacity for large scale manufacture and a commensurate savings with economies of scale. In this work a prototype trace sampling system intended for use with ion mobility spectrometers is presented. The system utilizes a stack of microfabricated preconcentrator plates capable of collecting samples in a sorbent polymer at flow rates up to 30 LPM. The plates are thermally desorbed after an integration period to produce a concentrated vapor plug that is transferred to the detector for analysis. A real-time controller, FPGA and custom electronics are used to manage independent heating of up to 4 of these devices in either constant voltage or temperature modes. The preconcentrators were tested with a commercial Vapor Tracer II IMS against TNT and RDX vapors ranging in concentration from 2.6 PPT to 620 PPT under a variety of conditions. Results are presented on performance of single preconcentrators with RDX, multiple cascaded devices vs. TNT and RDX, with and without a PDMS detector inlet membrane, and to compare sorbent coated and bare devices. The system demonstrated preconcentration factors of 38 with 2.6 PPT RDX and 30 with 13 PPT TNT.

Keywords Preconcentrator · Ion mobility spectroscopy · Trace detection · Micro-preconcentrator · MEMS

M. D. Martin (✉) · J. Aebersold · D. Jackson · K. Walsh · J.-T. Lin · M. G. O'Toole
Department of Electrical and Computer Engineering, University of Louisville,
Shumaker Research Bldg., Rm 237, 2210 S. Brook St., Louisville, KY 40208, USA
e-mail: michael.martin@louisville.edu

T. J. Roussel · S. Cambron · R. Keynton
Department of Bioengineering, University of Louisville, Louisville, KY 40208, USA

Introduction

The development of increasingly sensitive and portable analytical instrumentation has been aggressively pursued by university and corporate research for many decades, however until recently the focus on sample collection and pretreatment has lagged behind. In the last decade a number of important advances have demonstrated the application of MEMS technology to the field of sample collection. Often the methodology of MEMS sample collection takes the form of a thermal desorber that functions by collecting analyte at ambient temperature then releasing it at a second elevated temperature. In order to enhance collection efficiency and selectivity, a sorbent material is typically used within the collector or preconcentrator. These materials are often composed of porous zeolyte, carbon, modified PDMS or other polymers [1, 2]. MEMS fabrication techniques offer devices with a small physical footprint and low thermal mass resulting in low power consumption while rapidly reaching target temperatures. In some designs, as presented in this work, thin membrane style, flow-through preconcentrators allow for low pressure drops during the collection phase [3–7]. In many ways the plate style preconcentrators resemble solid phase micro-extraction (SPME) samplers and are well suited for trace detection of a narrow range of analytes [8, 9]. In other approaches, sorption bed style micro-preconcentrators [10–14] enable quantitative analysis of a broader range of

substances with wider dynamic range at the expense of sample flow rate, power consumption and desorption time.

The preconcentrators described here were designed for portable trace detection with ion mobility spectrometers (IMS), the most widely accepted technology for detection of illicit substances such as explosives, drugs of abuse and chemical agents [15, 16]. Therefore the devices were designed to minimize power consumption during collection and desorption events, provide a degree of analyte selectivity, and achieve a dynamic range sufficient to provide analyte above the detection limits of the IMS. To that end, the preconcentrators in this work are in a flow-through plate configuration; analyte is both collected and desorbed perpendicular to the collection surface. With sorbent material deposited on the plates as a polymer, this approach lends itself well to stacking the devices one atop the next for enhancing both collection efficiency and the breadth of analytes captured.

The preconcentrators were tested with a Vapor Tracer II, from GE Homeland Security. This instrument was chosen as it is widely deployed by the US Navy and as such is a useful metric for trace detection. A method for interfacing the micro-preconcentrators to the instrument is presented along with characterization versus TNT and RDX vapors. Operational characteristics were investigated to: elucidate device performance with a single plane and up to 4 stacked planes, optimize desorption temperature for TNT, compare constant temperature versus constant voltage desorption modes, compare coated versus uncoated preconcentrators and investigate desorptions with and without the PDMS inlet membrane attached to the Vapor Tracer II.

Design

The device is a variant of our previously reported preconcentrator design [3, 4, 6, 17]. It is composed of a 3 μm thick polyimide membrane, with two serpentine platinum heaters (35 μm wide×0.5 μm thick) on the top side and a 0.1 μm thick aluminum layer on the back, Fig. 1.

The perforations in the membrane form an array of 375 μm×125 μm rectangular openings to produce a ~42% open area fraction. The active area of the device is suspended on a silicon frame. The sorbent polymer (SC-F101 from Seacoast Science, Inc., Carlsbad, CA) is spray coated over the aluminum layer in the heated region of the device.

The devices were packaged for operation by a flip-chip bonding technique on to a custom printed circuit board. The flipped connection to the PCB enabled rugged stacking of devices using a second, spacer circuit board and a 90° rotation of each subsequent packaged preconcentrator. Electrical connection to each device was made with a standard card edge connector.

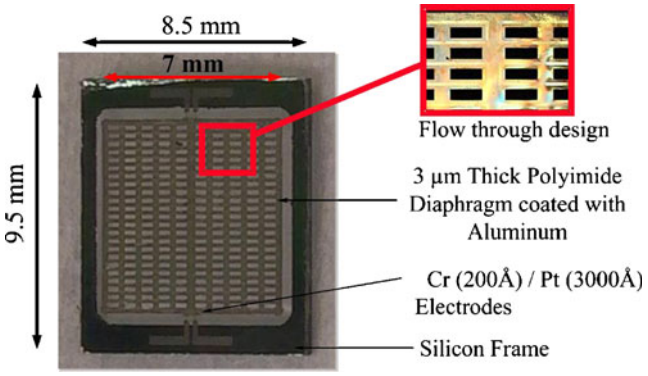

Fig. 1 Preconcentrator design

Experimental

Vapor generator

Tests were performed using a custom vapor generator that consisted of coiled double walled copper tubing used in the distillation of spirits. Two of these thermostated columns were connected together in a manifold with downstream mass flow controllers (MFC); the analyte column used a 0–200 SCCM MFC and the second column, used for diuent flow, had a range of 0–30 LPM. The inner sleeve of the analyte column was filled with 25 g of either TNT or RDX Non-hazardous Explosives for Security Training and Testing material (NESTT) from Van Aken, Inc., Los Angeles, CA. The exit of the vapor generator analyte column was plugged with silanized glass wool to prevent particles from leaving the thermostatic region. Control of the double walled tubing temperature was provided by recirculating water from a heater/chiller through the outer walls of the analyte and diluent columns. Sections of tubing downstream of the manifold were maintained within 4°C of the analyte column set point via heat tapes. In all experiments nitrogen gas was taken from the headspace of a liquid nitrogen dewar. The mass flow controllers and heater/chiller were controlled by a single LabView program.

The analyte column is assumed to produce a fully saturated vapor stream that follows the Dionne vapor pressure curves [18]. For TNT, the vapor pressure (P) in parts per billion is empirically related to the temperature by Eq. 1 and for RDX the pressure in parts per trillion is given by Eq. 2.

$$TNT : LogP(ppb) = -5481/T(K) + 19.37 \quad (1)$$

$$RDX : LogP(ppt) = -6673/T(K) + 22.5 \quad (2)$$

In practice it was necessary to idle the vapor generator for extended periods of time once a particular concentration and mixture were established before the output stabilized. This step was critical for the lower range of TNT vapor concentrations where it was necessary to let the vapor generator run for up to a day before IMS peak heights became constant.

IMS and calibration

The Vapor Tracer II utilizes Ni-63 for primary ionization of the reactive ion, dichloromethane, and features an internal calibrant of butylhydroxytoluene (BHT). In typical field applications the IMS utilizes a PDMS based inlet membrane heated to 200°C to partially isolate it from ambient conditions and interferents. In most experiments the membrane was removed so as not to impede the progress of the desorbed vapor plug and reduce the temporal resolution. The IMS further employs a cartridge of molecular sieve to minimize water vapor in the drift gas.

In order to estimate the preconcentration factors it was first necessary to calibrate the ion mobility spectrometer response versus explosives vapor concentration. The IMS was interfaced to the output of the vapor generator with a custom chuck that featured a bypass valve just before the IMS inlet to vent excess vapors. At each concentration the output of the vapor generator was allowed to stabilize for at least 1 hour before data collection. Figure 2a) illustrates the calibration curve for RDX versus IMS peak height without a PDMS inlet membrane on the IMS. The concentration in this data set was varied by changing the temperature of the vapor generator with a constant flow rate of 200 SCCM. At least 5 measurements were taken at each concentration and all data points are plotted. The shape of the curve illustrates that the instrument is optimized for trace detection as opposed to more quantitative measurements since its response asymptotically approaches a maximum peak height despite continued increase in analyte concentration over a relatively narrow dynamic range. Figure 2b) illustrates the data representing a similar TNT calibration without a PDMS membrane. The analyte concentration in these experiments was adjusted by using two different total flow rates (635 SCCM and 710 SCCM) and varying the vapor generator temperature from 5°C–25°C. The analyte flow was chosen to match the IMS sample pump flow rate (650±100 SCCM) so as to minimize pressure difference in the instrument. Despite this adjustment there is a shift in the sensitivity of the instrument from pressure effects. Figure 2c) illustrates TNT calibration with an inlet membrane. These data were taken at flow rates of 1.025 LPM–3.075 LPM and temperatures ranging

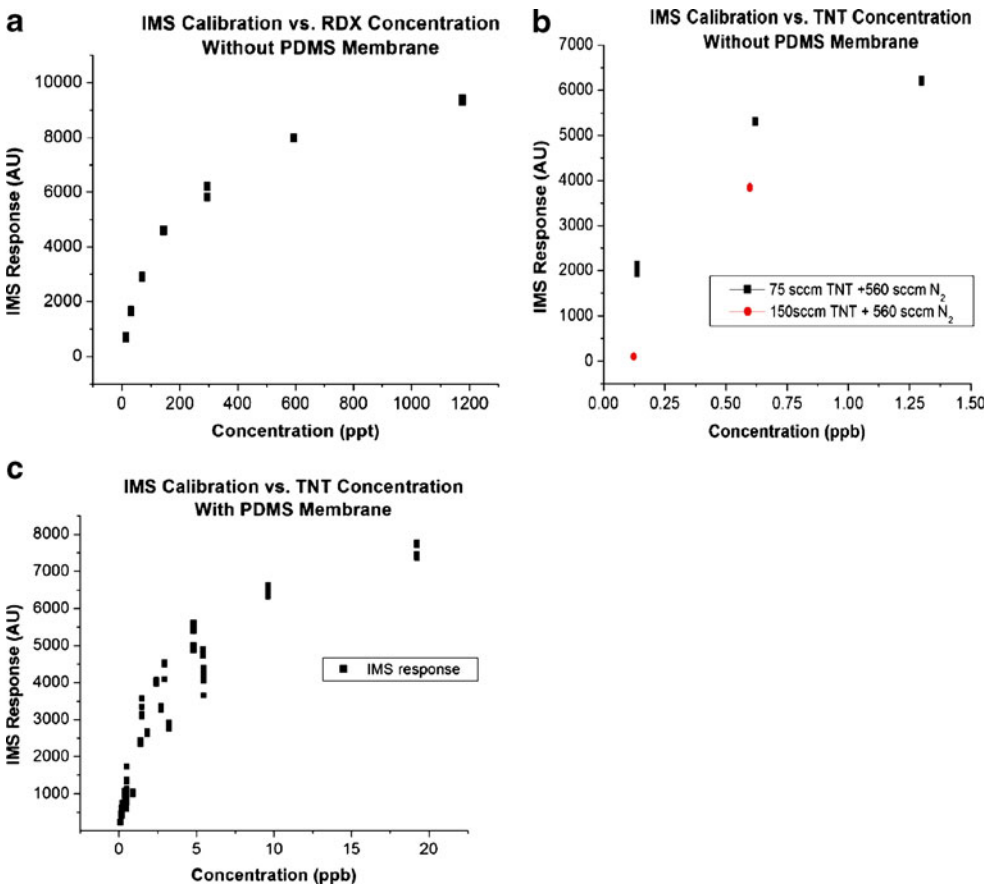

Fig. 2 IMS calibration versus **a**) RDX without PDMS membrane **b**) TNT without PDMS membrane and **c**) TNT with PDMS membrane

from 40°C to 10°C. Despite the variety of experimental conditions, the variation in the calibration curve is smaller than the case without a membrane and demonstrates the utility of using an inlet membrane to isolate the instrument from environmental effects.

Preconcentrator characterization and IMS interface

Once the devices are packaged, they are electrically characterized as detailed in [4] by measuring the resistance-temperature curve from 25°C to 180°C in an oven. The devices are then powered from 1 V to 22 V to determine the power-temperature relationship under zero flow conditions. Experiments with hundreds of these preconcentrators have shown the power-temperature relationship varies by less than 7% from device to device and is independent of the initial resistance of the device. The transient response is determined by applying a constant voltage sufficient to reach a steady state temperature of 120°C while measuring the time interval required to reach that temperature from 22°C. This interval is approximately 200 ms under an applied power of 175 mW, though it is possible to reach this temperature in <10 ms using a proportional, integral and derivative (PID) control algorithm.

The preconcentrators are interfaced to the IMS with a custom PEEK (polyether ether ketone) chuck defining a bypass flow path between the devices and detector inlet. Figure 3a) shows an exploded view of the chuck, preconcentrators and gaskets and Fig. 3b) illustrates the assembled part. The bypass valve is opened during the sample collection phase allowing arbitrary flow rates through the preconcentrators, independent of the IMS pneumatics. Before desorption the valve is closed and the IMS sample pump is used to pull analyte from the heated preconcentrators. In order to achieve efficient sample transfer between preconcentrators and IMS, the volume of the flow path is minimized and the tube walls are heated. Having the flow path heated is particularly critical for low vapor pressure analytes that rapidly settle out of the concentrated vapor plug. An aluminum sleeve defining this path was pressed into the PEEK chuck and is engineered so it is parasitically heated by the IMS inlet which is maintained at 200°C.

Preconcentration experiments were performed by attaching the IMS and preconcentrators to the vapor generator with a ½" compression fitting during sample collection with the bypass valve open. Desorptions were performed by removing the IMS from the vapor generator, closing the bypass valve and manually synchronizing the IMS sample pump flow with preconcentrator heating.

Hardware/software controller

The preconcentrators' operation is managed by a custom control program running on Compact Real-time I/O system (cRIO, National Instruments, Austin, TX) that features a 233 MHz Power PC and a 3 million gate field programmable gate array (FPGA). This platform offers flexibility through modular I/O units that plug into the cRIO's chassis and an operating system that provides microsecond timing resolution for deterministic control. The cRIO is interfaced to a voltage amplification circuit with a peak output voltage of 22 V and corresponding current measurement circuit to monitor each preconcentrator independently. Voltage modulation was chosen as opposed to pulse width modulation out of concern for the presence of short time constant hot spots on the devices.

Software for the controller is written in LabView and manages heating for up to four devices in either constant voltage or constant temperature/resistance mode. In either case, the current and resistance are plotted in real time which allows one to observe effects of flow, thermal crosstalk among stacked devices, and transient behavior during experiments. The user can set parameters for the proportional, integral and derivative control algorithm (PID), calibration constants for temperature conversion, and preconcentrator on time after a trigger event. Two set points are also provided in voltage and constant resistance

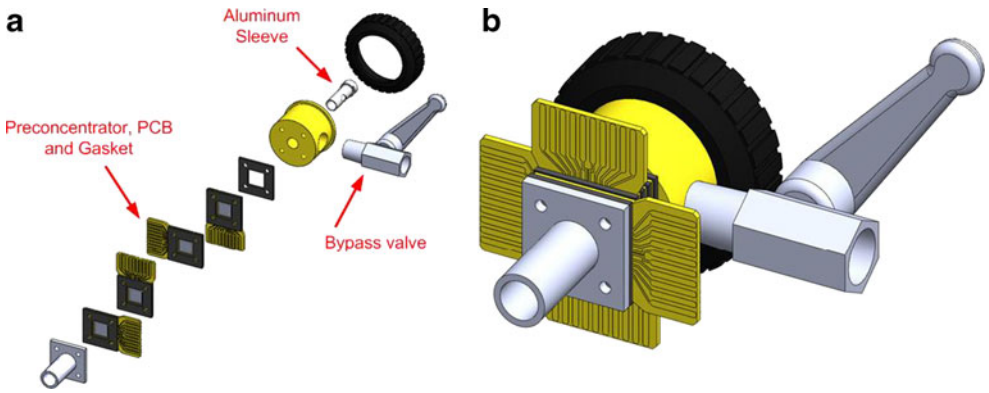

Fig. 3 **a** Exploded drawing of the preconcentrator chuck with 4 preconcentrators and **b** the assembled chuck

modes; one at the low end for idling the preconcentrators slightly above ambient temperature during sample collection and one for the desorption phase.

Results and discussion

Tests with individual preconcentrators

Initial experiments were performed with individual uncoated preconcentrator devices against RDX vapors. RDX was chosen since its low vapor pressure at ambient conditions (6 PPT [14], 10^{-9} Torr) translates to vapors that condense on uncoated devices as readily as the variety coated with a sorbent. This very property of RDX complicates its delivery from the preconcentrator to the inlet of the detector as the analyte plug will rapidly precipitate on any cool downstream tubing. In these experiments, the chuck discussed above was not yet fabricated so 14 PPT RDX vapors at 30°C were collected for 30 s at 190 SCCM by simply holding the device in front of the vapor generator outlet. After collection, the preconcentrator was manually held within 3 mm of the detector inlet and desorbed. Analyte release was manually synchronized with the sample pump of the IMS with no PDMS membrane. An example desorption event is shown in Fig. 4 where the device was heated for 2 s in constant voltage mode to 150°C (270 mW at zero flow). These data represent the raw spectra taken every 500 ms with total drift time of 15 ms that are averaged and curve fit to produce the "plasmagram" in the Vapor Tracer software. In the figure a background of RDX appears before and after the desorption event occurring from roughly 2 to 8 s in the integration time. This background may result from parasitic heating of the RDX contaminated silicon frame and printed circuit board by the heated detector inlet after manually holding the

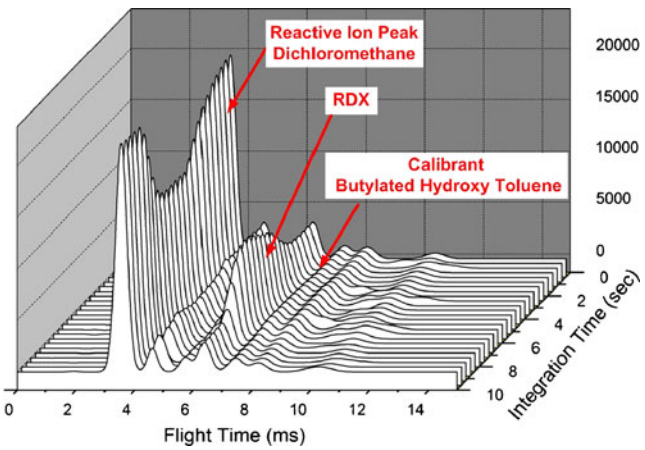

Fig. 4 Example desorption event for a single preconcentrator. The device was heated for 2 s in constant voltage mode to 150°C after 30 s collection of 14 PPT RDX

assembly in front of the vapor generator outlet. A series of desorption events showed an average RDX peak height of 6,734±1,293 (n=4). From the calibration, this peak height corresponds to a concentration of 400 PPT for a preconcentration factor of (400 ppt/14 ppt) 28.

In a second series of experiments the optimum desorption temperature was investigated once again without an inlet membrane though with the inclusion of a chuck. RDX vapor was collected at 143 PPT (45°C column temperature) for 30 s at 190 SCCM and then manually desorbed in constant voltage mode <1 s before engaging the sample pump at 130°C, 150°C and 175°C, as measured with zero flow, Fig. 5. At each temperature, five data points were taken and all are plotted in the figure. The data reflect that a temperature of at least 150°C was necessary to remove the bulk of the collected RDX though 170°C did not seem particularly detrimental to desorptions. Note that an average peak height of 3,500 (as occurs at desorption temperatures of 150°C or more) corresponds to roughly 120 PPT for a preconcentration factor of (143 PPT/120PPT) 0.84.

The time evolution of the analyte pulse was investigated in constant voltage and constant temperature modes with the desorption temperature set to 150°C, the sample pump was turned on within 1 s of heating the devices which were left hot until the pump shut off. In both modes, RDX was collected as above at 143 PPT, 190 SCCM, for 30 s. In Fig. 6 the spectra were taken from screen captures of the Vapor Tracer software in the "processed 3D" view and are essentially the same data representation shown in Fig. 4 but require much less effort to format and reproduce. The data on the left of the figure illustrates the RDX signal taken every 100 ms for constant temperature and on the right for constant voltage. The constant temperature curve monotonically increases and decreases whereas the constant voltage curve has an inflection point on the descending side of the pulse. The peak height obtained from the respective plasma grams (not shown) for the constant voltage spectrum was 4,033 and for constant temperature was 4,179.

Tests with stacked preconcentrators

RDX preconcentration, no membrane, uncoated devices

Initial tests with stacked preconcentrators were performed against RDX vapors with 3 uncoated devices at a desorption temperature of 170°C (300 mW) under constant voltage control. The IMS sample pump was started <1 s after heating the devices and no inlet membrane was used. Sample was collected from a vapor stream running at 5 LPM, 14 PPT (30°C) for 30 s through the bypass valve. Once the IMS and preconcentrators were removed from the vapor generator, IMS spectra indicated no RDX peak with the preconcentrators at ambient temperature (22°C). Spectra

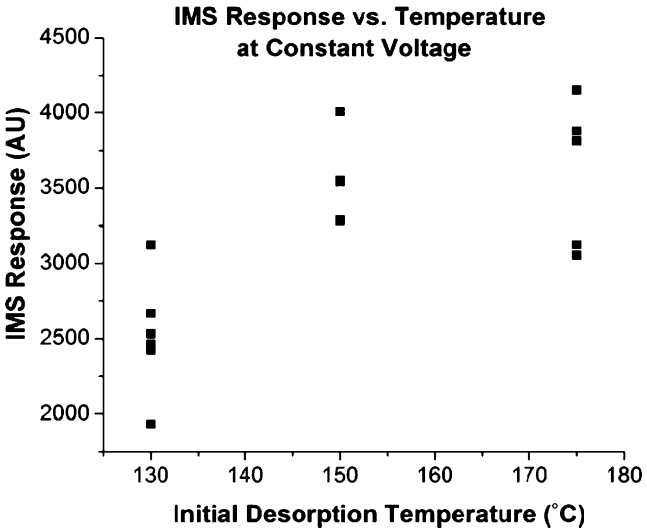

Fig. 5 Optimization of the desorption temperature with 30 s 142 PPT collection at 190 SCCM. Five data points were taken at each temperature

taken upon desorption of the three devices produced a RDX peak height of 3,434. From the RDX calibration curve this corresponded to ~70 PPT for a preconcentration factor of (70 PPT/14 PPT) 5. During the course of the desorption event there was significant depletion in the RIP as the RDX vapor plug reached a peak, thus saturating the instrument's response. The preconcentrators were left on after desorbing to clear the system of analyte: after 2 min the RDX peak height dropped to 257 and within 5 min all traces were gone.

Given the saturated nature of the 14 PPT RDX results, the concentration was reduced to 2.6 PPT RDX and analyte was collected on 4 uncoated devices at a flow rate of 5 LPM for 30 s with the vapor generator temperature at 20°C. Desorptions were performed at 170°C (300 mW) with the devices manually synchronized to fire no more than 1 s before the IMS sample pump. Several measurements produced an average peak response of 3,989±2,098 (n=3) which corresponds to a concentration of roughly 100 PPT from the calibration curve for a preconcentration factor of (100 PPT/2.6 PPT) 38.5. The large error in this measurement may be the result of the manual synchronization between preconcentrator desorption and initiation of detection within the IMS. An example desorption in Fig. 7 shows the rapid rise of the RDX signal followed by a gradual reduction of concentration as the series of spectra continues to 5 s. It was necessary to leave the devices hot for roughly 10 min before traces of RDX were removed from the system.

RDX preconcentration, with membrane, uncoated devices

A stack of 4 uncoated preconcentrators were tested with the PDMS membrane captured between the chuck and IMS inlet in an effort to elucidate its effects on preconcentrator performance. Analyte was collected on the devices at a concentration of 2.6 PPT and flow rate of 5 LPM for 30 s with the vapor generator temperature at 20°C. The spectrum shown in Fig. 8 is the result of a desorption at 170°C (300 mW). The IMS integration time (defined by GE as the period that 15 ms drift raw spectra are taken at a rate of 10/second) was set to 5 s to elucidate the time development of the analyte pulse into the detector. The desorption was manually timed so the devices were fired no more than a second before the sample was drawn into the IMS. It is clear from Fig. 8 that the temporal development of the analyte pulse

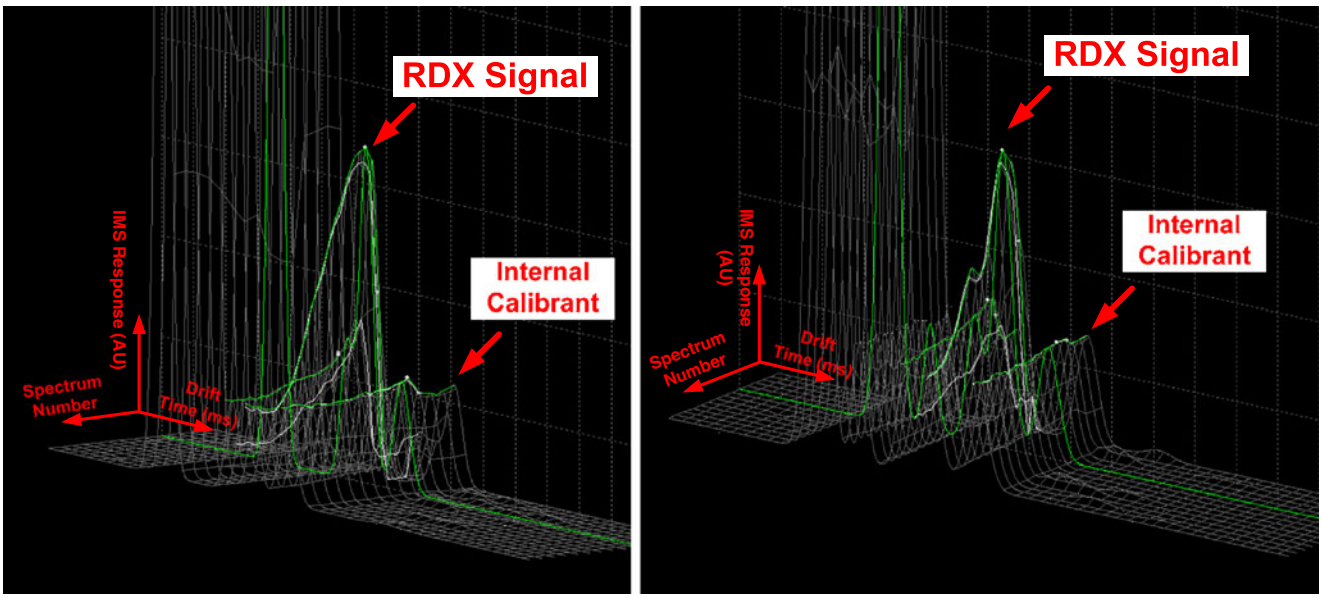

Fig. 6 Desorption of RDX at constant temperature (*left*) and constant voltage (*right*)

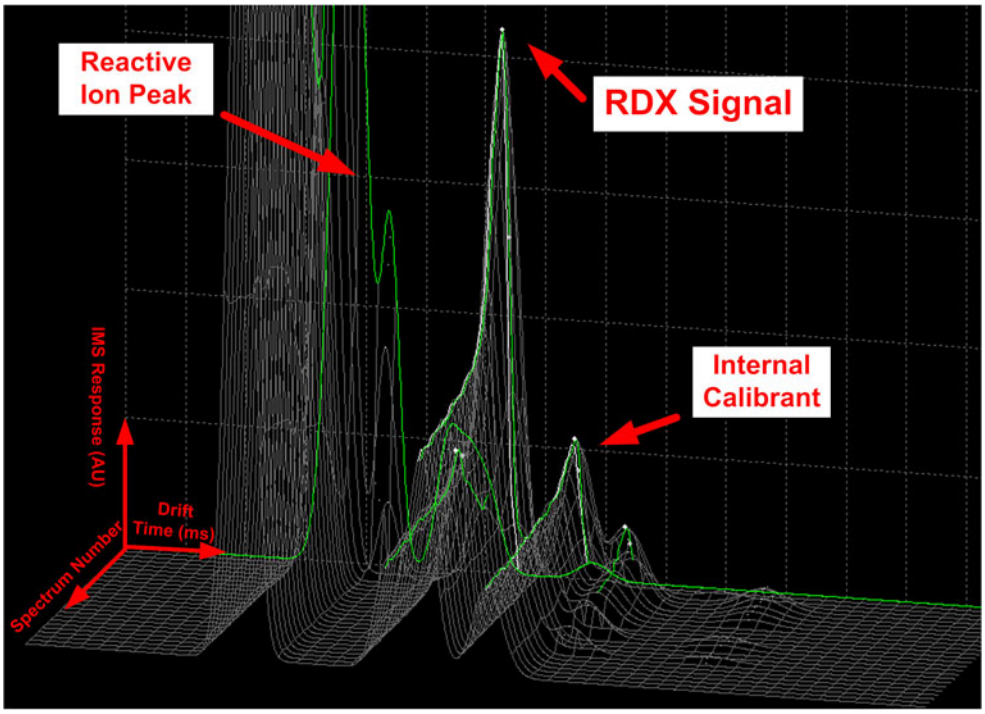

Fig. 7 Desorption of 4 uncoated preconcentrators without a membrane after collecting RDX vapors for 30 s at 2.6 PPT and 5 LPM

is not as sharp as without an entrance membrane. None the less, the averaged spectrum (plasmagram) indicated a healthy RDX peak at 6.583 ms with a peak height of 2,254. The lack of a calibration curve for RDX with a membrane precludes estimation of the preconcentration factor however a control spectrum with 2.6 PPT taken with the membrane but without the preconcentrators showed that this concentration is below the detection limit of the instrument, i.e. no peak was found.

TNT preconcentration, no membrane, uncoated devices

Experiments similar to the above were performed with 13 PPT TNT and three uncoated preconcentrators without an inlet membrane. The TNT vapor was produced at 10°C, 1.029 PPB and the analyte laden vapor stream running at 25 SCCM was diluted in 2 LPM N_2 for 13 PPT. Analyte was collected through the preconcentrators for 30 s at 2.025 LPM net flow rate. In order to verify that the sample was desorbing from the preconcentrators only, spectra were acquired with preconcentrators at ambient temperature but after sample collection. The spectra indicated no trace of TNT. The devices were desorbed at 170°C (300 mW) <1 s before engaging the IMS sample pump. A representative spectrum is shown in Fig. 9. There is a rapid rise in the TNT concentration as the analyte plug arrives and the TNT peak height from the plasmagram was 3,839. Due to the

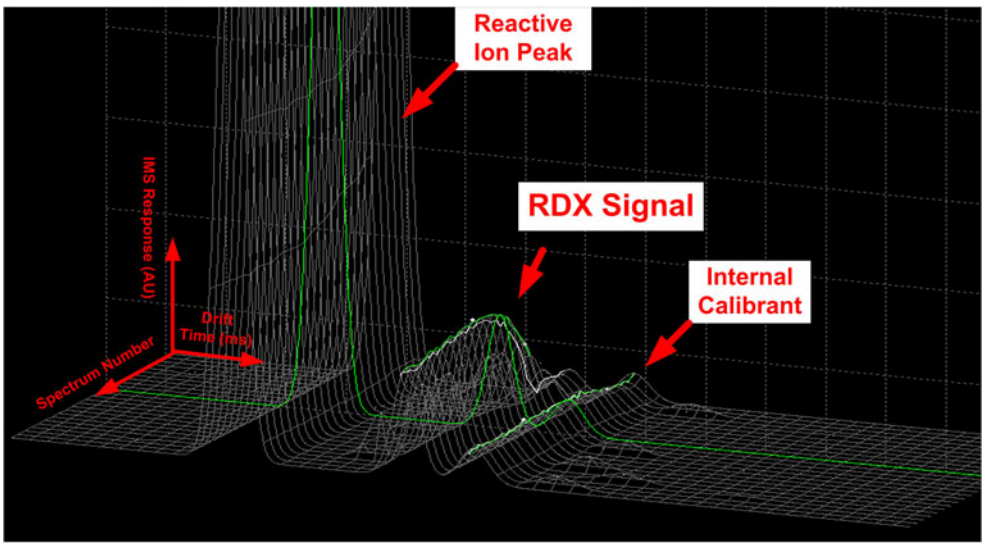

Fig. 8 Desorption of 4 preconcentrators through the inlet membrane after collecting 2.6 PPT RDX for 30 s at 5 LPM

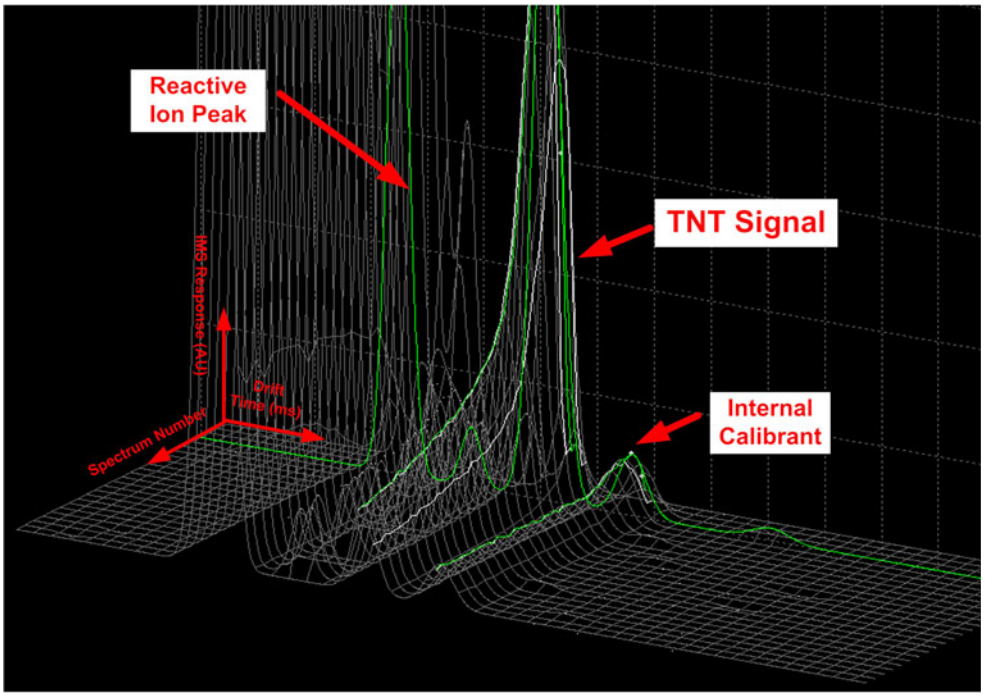

Fig. 9 Desorption after collecting 13 PPT TNT vapors for 30 s at 2.025 LPM

poor calibration for TNT without a membrane it is difficult to accurately measure the preconcentration factor however an estimate of 0.4 PPB would give (400 PPT/13 PPT) a preconcentration factor of 31. The devices were left on after desorption and 45 s later a second spectrum showed a TNT peak height of 186, well below the default alarm level of 250.

TNT preconcentration, no membrane, coated devices

A group of three coated preconcentrators were used to reproduce the above experiment. The devices were spray coated with SC-F101 polymer at Seacoast Science, Inc.. As initial tests with the devices indicated a number of unknown peaks assumed to be caused by interferents, it was necessary to purge the devices with 80°C nitrogen while leaving them at 120°C for 3 days before they were used in experiments. It was not clear whether the interfering compounds were the result of the polymer absorbing chemicals from the ambient lab environment or were coming from the polymer itself. Desorptions after collecting TNT for 30 s under the same conditions as above showed a peak height of 4,400 and a somewhat longer analyte pulse in the temporal development of the analyte plug. The lack of a proper calibration curve for TNT without an inlet membrane complicates calculation of the preconcentration factor however an estimate of 0.5 PPB would give (500 PPT/13 PPT) 38. Once again after leaving the devices on for 45 s, no TNT peak was found in the spectra, thus demonstrating effective clear down.

Further experiments were performed under the same collection conditions but under constant temperature (resistance) with the desorption temperature set to 150°C. Due to poor PID tuning the temperature of all the devices overshot the set point by at least 30°C resulting in the disappearance of the TNT peak at 6.164 ms and the appearance of a peak at 5.872 ms. This new peak was clearly associated with the preconcentrators given the temporal character and it was later determined that this peak was associated with the thermal decomposition of the polyimide.

TNT preconcentration, with membrane, coated devices

TNT preconcentration and analyte delivery was investigated using four coated preconcentrators with the IMS inlet membrane attached. TNT vapor was collected at a net concentration of 0.62 PPB from a diluted stream of pure TNT at 75 SCCM and 4.7107 PPB (20°C) with a net flow rate of 645 SCCM. A series of desorptions at 150°C (250 mW) after collecting for 30 s indicated an average peak height of 765±240 (n=3). An example of the time evolution of the released vapor through the membrane is shown in Fig. 10. As with RDX delivery through the membrane, the TNT signal does not rise as rapidly as the case without a membrane. Referring to the TNT calibration curve with a membrane, one would expect a concentration of 0.24 PPB for a peak height of 765 which results in a preconcentration factor of only (0.24/0.62) 0.39.

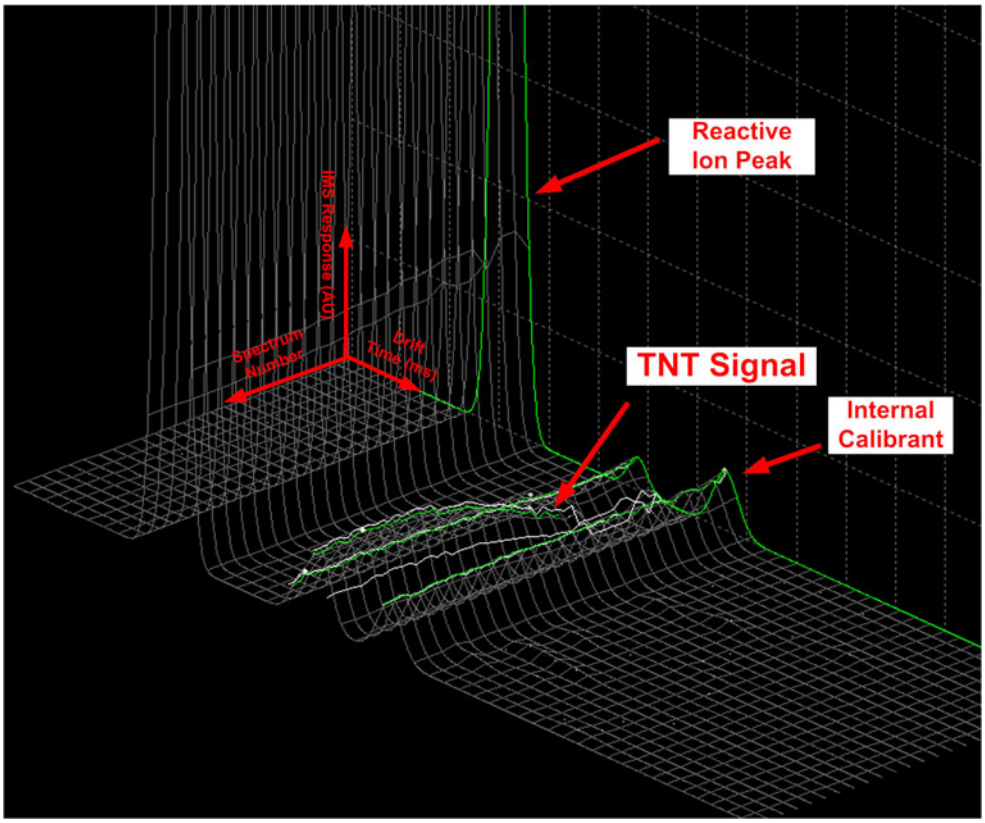

Fig. 10 Desorption from 4 coated preconcentrators through the inlet membrane after collecting for 30 s from a 0.62 PPB (20°C) TNT vapor stream at 645 SCCM

Summary of preconcentrator performance

The results of preconcentration factor measurements from the above experiments are summarized in Table 1. In all cases samples were collected from the vapor generator for a period of 30 s. The preconcentration factor is presented as a function of six variables though other effects such as timing variations and instrument saturation may have an impact. In general, the preconcentration factor seems to decrease as the analyte concentration rises. The infinity symbol (∞) is used for the case where using the preconcentrators reduced the detection limit of the instrument; that is the detector response without preconcentration at the challenge level was zero.

Conclusions

To facilitate testing of plate style flow-through preconcentrators, a custom vapor generator was built and used to calibrate the response of a commercially available IMS with TNT and RDX. The calibration versus TNT without a detector inlet membrane was found to be particularly problematic due to shifts in the detector sensitivity as a function of total analyte flow rate. These shifts appear to be caused by changes in the instrument's sensitivity as a function of pressure. This problem was not evident with RDX calibration as its wide range of volatilities enabled calibration by changing only the column temperature without changing the total flow rate and may have caused

Table 1 Summary of preconcentration factor measurements

Preconcentration Factor	Analyte and concentration	Collection flow rate	Membrane	Coated	Vapor temperature	Number of precons
28	14 PPT RDX	0.19 LPM	NO	NO	30°C	1
0.84	143 PPT RDX	0.19 LPM	NO	NO	45°C	1
5	14 PPT RDX	5 LPM	NO	NO	30°C	3
38.5	2.6 PPT RDX	5 LPM	NO	NO	20°C	4
∞	2.6 PPT RDX	5 LPM	YES	NO	20°C	4
31	13 PPT TNT	2.025 LPM	NO	NO	10°C	3
38	13 PPT TNT	2.025 LPM	NO	YES	10°C	3
0.39	620 PPT TNT	0.645 LPM	YES	YES	20°C	4

a systematic error in the calibration curve with respect to normal atmospheric operation. Comparing the IMS response versus TNT with and without the inlet membrane illustrates how effectively it decouples the instrument from ambient influences. One shortcoming with the measurements in general is that the output concentration is assumed to follow the Dionne curves however the calibration of the vapor generator should be cross checked by a more quantitative analytical technique such as GC/MS.

The chuck assembly with heated flow path seemed effective for transferring analyte between the preconcentrators and IMS inlet. The clear out of large analyte pulses and relatively sharp peaks produced during desorptions (Figs. 6 and 9) illustrate this point. However, it will be useful to measure the temperature of the aluminum flow path and its influence on analyte delivery to the detector. Indeed some of the desorption events for RDX (Fig. 7) show a significant RDX signal beyond the 5 s window of the data acquisition, indicating either incomplete desorption or adsorption on a cool downstream surface. It may therefore be useful to increase the temperature of this flow path and correct for temperature gradients therein.

The real time controller and FPGA were well suited to manage heating and data acquisition for up to 4 devices, allowing independent PID control with <10 μs timing. Synchronization between the preconcentrators and IMS was problematic however and some of the large measurement error for desorptions may be the result. A digital trigger input for initiating analyte release will be included in future versions of the controller hardware and software and should improve or eliminate synchronization problems.

Initial investigations using only a single preconcentrator without the interface chuck demonstrated the device was capable of taking a 14 PPT analyte stream and delivering it at 400 PPT. In some ways these experiments might be indicative of optimal delivery as no tubing was present to attenuate analyte between the preconcentrator and IMS. Further tests using an individual preconcentrator, mounted to the chuck, established that a minimum temperature of 150°C was necessary to fully desorb RDX; however increasing the target temperature to 170°C did not seem to be detrimental, i.e. no thermal decomposition was observed. Tests comparing the time evolution of the analyte pulse for constant temperature (PID) mode and constant voltage mode indicated a somewhat more uniform response for the constant temperature mode. However, this effect seemed to have little impact on the total analyte delivered as the RDX peaks in the spectra were of comparable height. In both the optimum desorption temperature tests and the constant voltage/temperature test, analyte was produced from a vapor at 142.6 PPT (45°C) and the preconcentration factor was less than one. This performance may be the result of losing analyte due to the preconcentrator reaching the temperature of the vapor stream thus collecting less efficiently. The devices may have also exceeded their capacity to collect analyte at this concentration resulting in little or no gain from the preconcentrator.

Tests with stacks of uncoated devices began with demonstration of RDX preconcentration using 14 PPT and resulted in a preconcentration factor of only 5. However, the significant depletion of the RIP and large analyte pulse obtained from 14 PPT RDX after 30 s collection likely distorted the peak reported in the averaged and peak fit spectrum of the plasmagram. This effect might be mitigated by ramping the desorption temperature so that the pulse is more spread out in time and lengthening the integration period. In an effort to avoid saturation of the detector's response the RDX concentration was reduced to 2.6 PPT and a preconcentration factor of 38.5 was achieved.

Tests at 2.6 PPT of RDX were performed with the inlet membrane on and resulted in a RDX peak height of 2,254. In comparison to the membraneless configuration the resulting analyte pulse width was much broader in time. In the future it will be useful to have a measurement of the full width at half maximum (FWHM) in the time domain to better quantify performance. Without a calibration curve for RDX with the membrane, a preconcentration factor cannot be presented and is clearly a necessity in the near term. However the use of the preconcentrators enabled the IMS to go from zero RDX signal to a very healthy peak thus demonstrating a substantial reduction in the detection limits.

TNT detection was initially investigated without an inlet membrane using uncoated preconcentrators at 13 PPT and demonstrated an approximate preconcentration factor of 30 from a peak height of 3,839 along with a sharply peaked analyte pulse as a function of time. This experiment was repeated with coated preconcentrators and a peak height of 4,400 was measured resulting in an estimated preconcentration factor of 38. These initial experiments suggest that the preconcentrators work well without a sorbent for the analytes tested. It may be that the polyimide comprising the device structural layer is acting as a sorbent as has been demonstrated for SPME in [9, 19].

TNT desorptions utilizing coated preconcentrators through the detector inlet membrane showed a clear broad signal similar to RDX desorption through the membrane. In this experiment the TNT vapor was collected at 0.62 PPB at a net flow rate of 645 SCCM for 30 s and resulted in a preconcentration factor of only 0.39. Further investigation is necessary to determine whether the poor performance may be the result of either saturating the devices, poor timing or attenuation through the membrane.

Further experiments are needed to investigate the preconcentrators' capacity to absorb analyte as a function of mass from the vapor phase and should further explore this capacity in a wider variety of coatings and compounds.

It will be useful to further explore the ability of the devices to hold onto analyte under experimental conditions intended to model security screening applications. Specifically, a brief pulse or particle of analyte will be collected in the preconcentrators followed by a relatively large volume of diluent as might happen in passenger, baggage or vehicle screening. Though better statistics will be necessary to elucidate a number of operational characteristics; in general the preconcentrators show promise for improving the performance of near real-time detectors and analytical instrumentation, potentially in a wide variety of applications and for many other classes of analytes.

Acknowledgments The authors would like to thank David Hollinberger and Jack Fulton of NSWC Crane for their support and valuable guidance. We would also like to thank Jennifer Stepnowski and Andrew McGill of the Naval Research Laboratory for help with initial RDX testing and advice about coatings. This work was supported by the U.S. Navy under Contract DAAB07-03-D-B010/TO-0198. Technical program oversight was provided by Naval Surface Warfare Center, Crane Division. Further support was provided by the Department of Justice (2004-IJ-CX-K055), the Critical Infrastructure Assurance Office Protection, Department of Homeland Security and the Kentucky Department of Home Town Security.

References

1. Supelco Technical Report, A tool for selecting an adsorbent for thermal desorption applications. http://www.sigmaaldrich.com/etc/medialib/docs/Supelco/General_Information/t402025.Par.0001.File.tmp/t402025.pdf
2. Houser EJ, Mlsna TE, Nguyen VK, Chung R, Mowery RL, McGill RA (2001) Rational materials design of sorbent coatings for explosives: applications with chemical sensors. Talanta 54:469–485
3. Martin M, Crain M, Walsh K, McGill RA, Houser EJ, Mott D, Stepnowski J, Stepnowski S, Nguyen V, Wu H-D, Ross S, Nagel DJ, Voiculescu I (2004) Development of a microfabricated vapor preconcentrator for portable ion mobility spectroscopy. Solid-State Sensor, Actuator and Microsystems Workshop, Hilton Head Island, SC, USA, pp 390–391
4. Martin MD, Crain MM, Walsh KM, McGill RA, Houser EJ, Stepnowski JL, Stepnowski SV, Wu H-D, Ross SK (2007) Microfabricated vapor preconcentrator for portable ion mobility spectroscopy. Sens Actuators B–Chem 126(2):447
5. Voiculescu I, McGill RA, Zaghloul ME, Mott D, Stepnowski J, Stepnowski S, Summers H, Nguyen V, Ross S, Walsh K, Martin M (2006) IEEE Sens J 6:1094
6. McGill RA, Stepnowski SV, Houser EJ, Simonson DL, Nguyen V, Stepnowski JL, Mentzer H, Rake M, Martin M, Walsh K, Aebersold J, Ross SK (2006) CASPAR, a microfabricated preconcentrator for enhanced detection of chemical agents and explosives. Proc. of Eurosensors XX, Goteborg, Sweden
7. Voiculescu I, Zaghloul M, Narasimhan N (2008) Microfabricated chemical preconcentrators for gas-phase microanalytical detection systems. Trends Anal Chem 27(4):327
8. Belardi RG, Pawliszyn J (1989) The application of chemically modified fused silica fibers in the extraction of organics from water matrix samples and their rapid transfer to capillary columns. Water Pollut Res J Can 24:179
9. Arthur CL, Janusz Pawliszyn (1990) Solid phase microextraction with thermal desorption using fused silica optical fibers. Anal Chem 62(19):2145–2148
10. Yeom J, Field CR, Bae B, Masel RI, Shannon MA (2008) The design, fabrication and characterization of a silicon microheater for an integrated MEMS gas preconcentrator. J. Micromech. Microeng. 18, 125001, pp 12
11. Zellers ET, Steinecker WH, Lambertus GR, Agah M, Lu C-J, Chan HKL, Potkay JA, Oborny MC, Nichols JM, Astle A, Kim HS, Rowe MP, Kim J, da Silva LW, Zheng J, Whiting JJ (2004) Proc. Solid-State Sens., Actuator Microsyst. Workshop, Hilton Head, SC, USA, 6–10, pp 61–66
12. Tian W-C, Pang SW (2003) Thick and thermally isolated Si microheaters for microfabricated preconcentrators. J Vac Sci Technol B 21:274–279
13. Tian W-C, Pang SW, Lu C-J, Zellars ET (2003) Microfabricated preconcentrator-focuser for a microscale gas chromatograph. J Microelectromechanical Syst 12:264–272
14. Ruiz AM, Gracia I, Sabate N, Ivanov P, Sanchez A, Duch M, Gerboles MF, Moreno A, Cane C (2007) Membrane-suspended microgrid as a gas preconcentrator for chromatographic applications. Sensors Actuators A 135:192–196
15. Ewing RG, Atkinson DA, Eiceman GA, Ewing GJ (2001) A critical review of ion mobility spectrometry for the detection of explosives and explosive related compounds. Talanta 54:515–529
16. Baumbach JI, Eiceman GA (1999) Ion mobility spectrometry: arriving on site and moving beyond a low profile. Appl Spectrosc 53(9):338A–355A
17. Pai RS, McGill RA, Stepnowski1 SV, Stepnowski JL, Williams KP, Summers H, Furstenberg R, Rake MT, Nguyen VK, Simonson DL, Higgins B, Kendziora C, Houser EJ (2007) Towards enhanced detection of chemical agents: design and development of a microfabricated preconcentrator. Transducers & Eurosensors '07, 14th Int. Conf. Solid-State Sensors, Actuators and Microsystems, Lyon, France, pp 2291–2294
18. Dionne BC, Rounbehler DP, Achter EK, Hobbs JR, Fine DH (1986) Vapor presure of explosives. J Energ Mater 4:447–472
19. Ding T-H, Lin HH, Whang CW (2005) Determination of chromium(III) in water by solid phase microextraction with a polyimide-coated fiber and gas chromatography-flame photometric detection. J of Chromatography A 1062:49–55